DC Transport in Gubser-Rocha Holographic Matter

Post, Johannes

DC Transport in Gubser-Rocha Holographic Matter

Thesis

submitted in partial fulfillment of the
requirements for the degree of

Master of Science
in
Physics

Author :	Johannes Post
Student ID :	s2033429
Supervisor :	Prof. dr. K. Schalm
Second corrector :	Prof. dr. J. Zaanen

Leiden, The Netherlands, June 30, 2022

DC Transport in Gubser-Rocha Holographic Matter

Johannes Post

Instituut-Lorentz, Leiden University
P.O. Box 9500, 2300 RA Leiden, The Netherlands

June 30, 2022

Abstract

In the past decades experiments have found condensed matter systems which could not be described by the conventional methods of condensed matter theory, these are densely entangled strange metals. During the same period, the string theory community has developed the AdS/CFT correspondence, a duality between field theories and gravitational systems. This duality may be used to understand condensed matter field theory from a gravitational perspective. It is especially useful for densely entangled quantum matter, which can be described according to the duality by charged black hole systems of classical gravity. In this thesis we will consider the Gubser-Rocha black hole of the Einstein-Maxwell-Dilaton action to describe a metal. To understand charge and heat transport in these metals, one needs a mechanism to dissipate momentum. This is explicitly implemented by introducing a periodic lattice in the condensed matter system. Using heavy numerical codes to calculate the gravitational differential equations that are dual to the metal, we can find the transport properties of our metal. In this metal a linear in T resistivity is found, which is a famous property of the strange metals. Furthermore we find empirically a saturation of the conductivity, which could be the instance of Planckian dissipation and the minimal viscosity of the strange metal.

Contents

Chapter 1

Introduction

Condensed matter physics and quantum gravity seem to be different physical area's, located on the opposite side of the physics 'landscape'. Physicists are exploring the realms of quantum gravity, but have not yet settled on a complete and consistent theory. Perhaps the foremost theory that is being research is string theory. At the same time, condensed matter physicist are searching for a theory explaining the strange metal behavior discovered in experiments. Motivated by the discovery of high temperature superconductivity and the efforts of the string theory community, we are discovering that these seemingly different area's of physics are related in an unexpected way.

In 1911 in Leiden, Kamerlingh Onnes saw in his experiments that the resistivity of mercury at 3K is practically zero [1], discovering superconductivity. The first theory successfully describing this phenomenon is BCS theory [2, 3]. Proposed by Bardeen, Coop and Schrieffer (BCS) in 1957, they explained that for any attractive potential in a metal, below a critical temperature T_c the fermions will condensate into pairs, called Cooper pairs. These pairs have bosonic properties and will be protected by the collective condensate and may flow without resistance: superconductivity. Superconductors that may be described by BCS theory are what we call *conventional superconductors*. These metals typically have a T_c lower than $30K$ [4–6], however playing with light elements and high pressures also higher temperatures can be achieved. For example, metallic hydrogen under high pressure is expected to have a high T_c according to BCS theory [7], and high T_c of 203K consistent with BCS theory have been experimentally achieved in hydrogen-based metals [8]. Superconductivity which cannot be explained by BCS theory, is referred to as *unconventional superconductivity*. In 1986 Bednorz and Müller discovered high temperature superconductivity in copper-oxides (cuprates) at $T_c = 35K$ [9], which could not be explained by BCS theory. Up to that moment superconductivity had only been found below $30K$, marking their experiment as among the most important discoveries of the last century [6]. In the years following, other cuprates and different materials were found to have a superconducting phase at even higher temperatures.

Classical condensed matter field theory revolves around perturbation theory. The idea is that the macroscopic state can be described by a short range entanglement (SRE) state: a state with finite overlap with a state which is a superposition of single particle wave packets [10, 11]. This state of classical particles is an exact eigenstate of the Hamiltonian

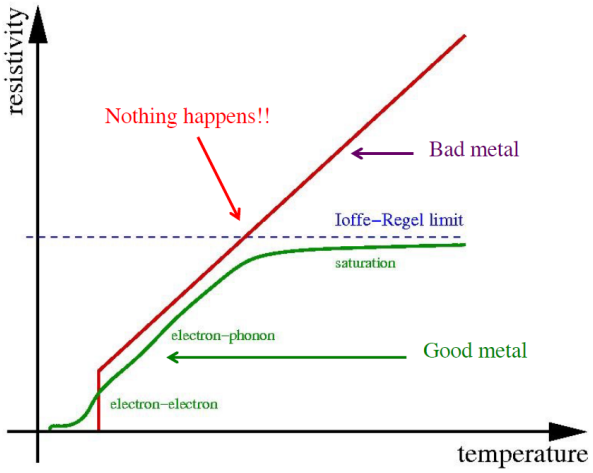

Figure 1.1: *The linear in T resistivity of a strange metal does not saturate like the resistivity of a Fermi liquid. Figure retrieved from [11].*

and therefore an exact state in our Hilbert space. Dressing this classical ground state by entanglements in a perturbative manner, we arrive at the so called SRE state. Although not an exact eigenstate, this state is quite well localized in Hilbert space, due to its finite overlap with the classical ground state, keeping the perturbation theory convergent.
This however, only works well when the couplings are small, by which we mean small enough such that the perturbation theory still converges. For large couplings, the perturbation theory will diverge and the methods of condensed matter field theory fail to tackle the problem. BCS theory and the Fermi liquid are results of perturbative condensed matter theory. Metals with strong electron interactions can not be described in a perturbative manner, due to the magnitude of their coupling. Superconductivity arising in these type of metals will therefore not be of the conventional kind.

The discovery of superconductivity in cuprates, was the discovery of the first strange metals. Strange metals are metals which cannot described by classical condensed matter field theory, and they have 'strange' or non-classical behavior. High T_c superconductivity is an example of those behaviors, but these same systems also have different properties at temperatures above T_c outside the superconducting phase. Another important property found in strange metals is the linear in temperature resistivity $\rho \sim T$, see Figure 1.1. The Fermi liquid has $\rho \sim T^2$ at very low temperatures where the resistivity is dominated by electron scattering. As the temperature rises, the electron-phonon interactions become more important and the resistivity becomes approximately $\rho \sim T$. However as the temperature rises more and the resistivity increases, the mean-free path which the electrons travel will become of the order of the lattice spacing. We run into the Mott-Ioffe-Regel limit: the resistivity will saturate. Strange metals however do not experience such a saturation. Above the superconducting phase, they experience a linear in T resistivity, up to temperatures where the metal becomes unstable and melts.

The strange behavior is believed to be related to quantum criticality. A quantum phase transition can happen at zero temperature, creating a sense of order in the system. Such transitions are characterized by universality and scale invariance. But even at non-zero temperatures, the system knows about the quantum critical point and can characterize

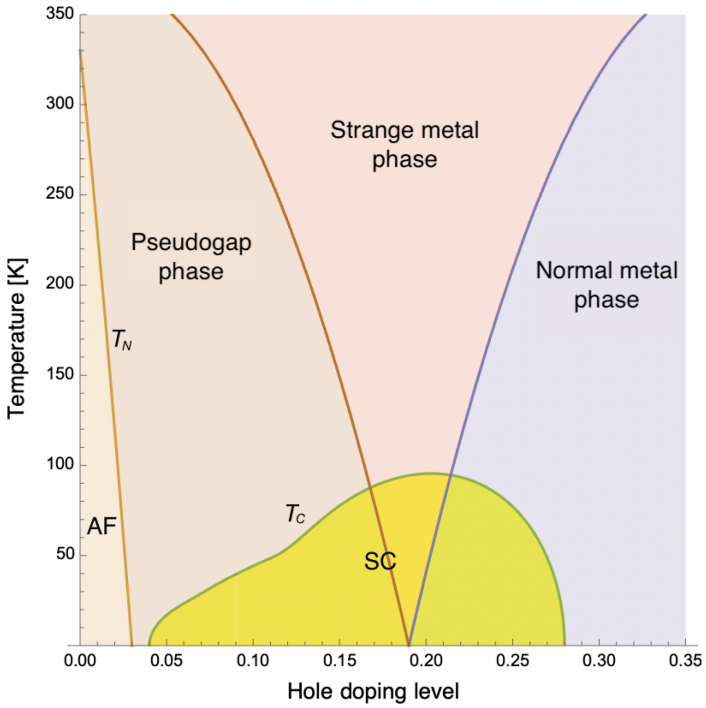

Figure 1.2: *Phase diagram of cuprates. Above the quantum critical point, we see the quantum critical wedge of the strange metal phase. Figure retreived from [12].*

the strange metals phase. This is the famous quantum critical wedge which can be seen in Figure 1.2.

In 1997 Maldacena discovered that field theories may be described by a gravitational theory in one higher dimension: the AdS/CFT correspondence [13]. This result from string theory offers a new approach for condensed matter physics. The discovery appears to be especially useful for the strongly coupled strange metals, where charged black holes can be used to describe finite temperature and finite density strange metals, which is currently the topic of interest in the Leiden Quantum Matter Theory Group. To account for charge and heat transport in metals, a lattice must be introduced in the metal. Introducing a lattice however makes the equations of the black hole system even more complicated and computational efforts are needed to do the calculations. This thesis will be the natural follow up on the theses of Sam Arend [14] and Martijn Janse [15]. They considered transport in Einstein-Maxwell theory with a Reissner-Nordström (RN) black hole, including magnetic fields. RN is known to produce some nonphysical results such as zero-temperature entropy. To go from this phenomenological system to a more physical representable system one must add a dilaton field. This solves the zero temperature entropy and is called Einstein-Maxwell-Dilaton (EMD) theory. In this thesis we will consider the Gubser-Rocha (GR) black hole in EMD, however without magnetic field, as including the dilaton field will increase computational difficulty.

After going over some classical condensed matter physics in Chapter 2, the correspondence and its application to finite temperatures and densities will be explained in Chapter 3. In Chapter 4 the application of the correspondence to condensed matter is discussed. Then the setup for the calculations is set out in Chapter 5, of which the results are presented

in Chapter 6. The thesis will be concluded with a discussion in chapter 7.

Chapter 2

Condensed Matter Physics

Condensed matter physics attempts to explain the physical properties of matter. Metals are of specific interest, as they may transport heat and electricity. In this chapter we will introduce some basic concepts of condensed matter physics. Section 2.1 starts off with the basics of transport responses. Drude theory is a model for transport based on momentum relaxation as explained in Section 2.2. This is followed by a short description of the Fermi liquid in Section 2.3, a model for conventional metals. Condensed matter systems are generally hard to described. Nevertheless condensed matter theory has a successful approach in providing descriptions of many metals. In Section 2.4 it is explained from a quantum information viewpoint why this is the case and also how this approach limited.

2.1 Transport

If a physical quantity sources a physical current, it can be described by linear response theory. In the Fourier domain the relationship between the source and current is captured by a Green's function called the response function (or sometimes susceptibility in physical context). An electrical current is sourced by an electric field. The relationship between electric current $\vec{J}$ and electric field $\vec{E} \sim -\nabla\mu$ is famously known as Ohm's law $\vec{J} = \sigma\vec{E}$, where the response function σ is known as the electric conductivity. However considering metals, we can also consider a heat current Q. A temperature gradient ∇T in a metal may cause heat transport and thus source the heat current. This is captured by the thermal conductivity $\bar{\kappa}$ as $Q = -\bar{\kappa}\nabla T$. Considering the particles carrying charge may also carry entropy, they may also cause a heat current. For that reason an electric field may also source heat currents and temperature gradients may cause electrical currents. These effects are captured by the thermo-electric conductivities α and $\bar{\alpha}$ as

$$\begin{pmatrix} \vec{J} \\ \vec{Q} \end{pmatrix} = \begin{pmatrix} \sigma & \alpha T \\ \bar{\alpha} T & \bar{\kappa} T \end{pmatrix} \begin{pmatrix} \vec{E} \\ -\frac{\nabla T}{T} \end{pmatrix}. \tag{2.1}$$

Due to the Onsager reciprocal relations, the the heat current induced by an electric field should be equal to the electrical current induced by the temperature gradient: $\alpha = \bar{\alpha}$ [16].

In this thesis we will consider two more directly related quantities,

$$\sigma_{Q=0} = \sigma - \frac{\alpha T \bar{\alpha}}{\bar{\kappa}}\,, \tag{2.2}$$

$$\kappa = \bar{\kappa} - \frac{\alpha T \bar{\alpha}}{\sigma}\,. \tag{2.3}$$

Here $\sigma_{Q=0}$ is the electric conductivity at zero heat current. Consider a system with charge conjugation symmetry, for example a metal with an equal amount of positive and negative charges. If we apply an electric field, all positive charge carriers will move in the direction of the field, while the negative cariers will travel in opposite direction. The currents caused by both the negative and positive carriers will result in an electric current in the same direction. If these charge carriers also carry entropy, we will have two opposing heat currents canceling each other out. The result is a system in which the electric current can exist without macroscopic heat transport: the electrical current has completely decoupled from the total momentum. However not all metals have charge conjugation symmetry. Nevertheless, we can come up with an alternative system that includes both neutral and positive charge carriers. If we then turn on an electric field, the positive charges will start moving. In addition a temperature gradient is turned on, slowing down the positive charges and accelerating the neutral carriers in such a way that the thermal transport of the two cancel each other. We will not have macroscopic heat transport, but we will have charge transport. From (2.1) we find that this happens if $\nabla T = \frac{\bar{\alpha}T}{\bar{\kappa}}\vec{E}$, which results in $\vec{J} = \left(\sigma - \frac{\alpha T \bar{\alpha}}{\bar{\kappa}}\right)\vec{E} = \sigma_{Q=0}\vec{E}$. Analogously, κ is the thermal transport at zero electric current. We can come up with analogous example for thermal transport without electrical currents. We should then find a heat current which slow the charged particles to a halt, such that the resulting system has no charge transport. There is however no simple interpretation for this in system with charge conjugation symmetry.

2.2 Drude Theory

Drude theory is a simple model to describe the conductive properties of metals, as can be found in any undergraduate textbook on condensed matter or solid state physics (e.g. [17]). Despite the simplifications and approximations taken by Drude theory, the model achieves a powerful description of electron transport. The model considers momentum carrying the electric currents. This can easily be understood from the particle viewpoint. Take classical electrons losing momentum due to scattering, characterized by the scattering time τ. The response of the electrons due to electric and magnetic fields must also be taken into account. This yields the following effective equation for the electron momentum:

$$\frac{d\mathbf{p}}{dt} = -e(\mathbf{E} + \frac{\mathbf{p}\times\mathbf{B}}{m}) - \frac{\mathbf{p}}{\tau}\,, \tag{2.4}$$

where $\mathbf{p} = \langle \mathbf{p}(t) \rangle$. This is the starting point of Drude theory. Consider the linear response and substitute $\mathbf{j} = -ne\mathbf{v} = -ne\frac{\mathbf{p}}{m}$, where n is the electron density. For $B = 0$ one simply finds

$$\mathbf{j}(\omega) = \sigma(\omega)\mathbf{E}(\omega) = \frac{\omega_p^2}{\frac{1}{\tau} - i\omega}\mathbf{E}\,, \tag{2.5}$$

Version of June 30, 2022– Created June 30, 2022 - 14:02

where $\omega_p^2 = \frac{e^2 n}{m}$ is the plasmon frequency. However we also wish to include the magnetic field, thereby promoting σ to a matrix. Consider the case where the magnetic field is perpendicular to the electric field. Taking the magnetic field in the z-direction, $\mathbf{B} = B_z \hat{z}$ and the electric field in the x,y-plane, $\mathbf{E} = E_x \hat{x} + E_y \hat{y}$. By defining the cyclotron frequency as $\omega_c = \frac{eB_x}{m}$, these equations can be rewritten in the form

$$\begin{aligned} \frac{dP_x}{dt} + \frac{1}{\tau} P_x &= eE_x + \omega_c P_y \\ \frac{dP_y}{dt} + \frac{1}{\tau} P_y &= eE_y - \omega_c P_x \,. \end{aligned}$$

However if we allow for a difference in the longitudinal an transversal scattering, we will find the more general equations:

$$\begin{aligned} \frac{dP_{x,L}}{dt} + \frac{1}{\tau_L} P_{x,L} &= eE_x \,, & \frac{dP_{y,L}}{dt} + \frac{1}{\tau_L} P_{y,L} &= eE_y \,, \\ \frac{dP_{x,T}}{dt} + \frac{1}{\tau_T} P_{x,T} &= \omega_c P_y \,, & \frac{dP_{y,T}}{dt} + \frac{1}{\tau_T} P_{y,T} &= \omega_c P_x \,. \end{aligned}$$

where $P_{x/y} = P_{x/y,L} + P_{x/y,T}$. Now we consider again an oscillating field $E(t) = Ee^{-i\omega t}$, we find for the conductivity

$$\begin{aligned} \sigma_{xx} &= \frac{\omega_p^2}{\left(\frac{1}{\tau_L} - i\omega\right)\left(1 + \frac{\omega_c^2}{\left(\frac{1}{\tau_T} - i\omega\right)^2}\right)} \\ &= \frac{\omega_p^2}{\left(\frac{1}{\tau_L} - i\omega\right)\left(1 + \left(\frac{\sigma_{xy}}{\sigma_{xx}}\right)^2\right)} \,, \\ \sigma_{xy} &= \sigma_{xx} \frac{\omega_c}{\frac{1}{\tau_T} - i\omega} \,, \end{aligned}$$

where we emphasize that τ_L and τ_T need not to be equal. As we can see from (2.4) and (2.5), the particle viewpoint is not necessary, only the coupling between momentum and electric currents matters.

2.3 Fermi Liquid

Drude theory only describes currents due to momentum relaxation in metals and does not take into account some basic principles of quantum theory, such as the Pauli exclusion principle. Normal metals are best described in condensed matter field theory by the Fermi Liquid. To understand the Fermi liquid, one must start out with the Fermi gas. The Fermi gas is a gas of non-interacting fermions in an infinite d-dimensional square well. In the ground state of the Fermi gas, the fermions occupy all states below the Fermi energy, or similarly all states below the momentum space Fermi surface at $k = k_F$:

$$|\Psi\rangle = \prod_{k=0}^{k_F} c_k^\dagger \, |vac\rangle \,, \tag{2.6}$$

where $c_k^\dagger$ is of course the fermion creation operator. Since fermions obey Fermi-Dirac statistics, one can derive the thermodynamic quantities for a large Fermi gas in thermal equilibrium. A Fermi liquid also takes into account weak fermion-fermion interactions. The Fermi liquid is equivalent to a Fermi gas of quasiparticles, where the quasiparticles have effective properties (such as effective mass and effective charge) to account for the fermion-fermion interactions. The important scale for the properties in the Fermi liquid is the Fermi energy E_F, the Fermi liquid is therefore not a quantum critical system, since the IR of a quantum critical system has no knowledge of any scale. The scattering time of the Fermi liquid quasi-particles is $\tau \simeq \frac{E_F}{k_B T}\tau_\hbar \sim T^{-2}$. Therefore the resistivity will scale as $\rho \sim T^2$, in the low temperature regime where particle scattering dominates. Furthermore, the Fermi liquid has a Sommerfeld entropy $S \sim \frac{k_B T}{E_F}$.

2.4 Where Condensed Matter Field Theory Fails

Given the Hamiltonian of a system of N particles, the eigenstates will be of the form

$$|\Psi\rangle = \sum_{i=0}^{2^N} a_i |\psi_i\rangle \ , \tag{2.7}$$

where the upper limit of the summation is 2^N, since this is the dimension of the Hilbert space of N qubits. We see that this is of exponential complexity. The type of problems that one can solve within a reasonable computation time are of polynomial complexity. The exponential complexity of (2.7) is beyond polynomial complexity, meaning that we can typically not solve this for large N.

The reason why there is nevertheless a successful description of many condensed matter systems, is that they are of a special type. These systems have a ground state dominated by a classical state, which can perturbatively be dressed up by quantum entanglements: [10, 11]

$$|\Psi_0\rangle = A \left|\psi_0^{classical}\right\rangle + \sum_i a_i |\psi_i\rangle \ . \tag{2.8}$$

Here $A \gg a_i$ and only some a_i are non-zero. We refer to such wave functions as Short Range Entanglement (SRE) tensor product states. The classical state is a simple tensor product, for example a product of single particle states. The unentangled classical ground state gets dressed up with entanglements in a perturbative manner. Due to the finite overlap of the ground state with the classical state, this state stays well localized in some degree of freedom (e.g. location or momentum) in the Hilbert state. This keeps the perturbation theory convergent and therefore of polynomial order. Examples are the Fermi Liquid and the BCS ground state. For the Fermi liquid, the Fermi gas (2.6) works as an anchor, keeping the full state well localized in Hilbert space. Particles as we know them are described as excitations of the vacuum. The vacuum is described by quantum numbers associated with the conserved quantities of the system. A particle excitation is just a different set of these quantum numbers, such that this state is well localized in Hilbert space. This means that particles as we know them require the system to be of the SRE form (2.8). For this reason we may refer to the non-SRE many body entangled physics as unparticle physics. [18]

There is yet another type of state for which condensed matter physicists have found a successful description: stoquastic systems. Under the right conditions, the ground state of a strongly interacting quantum critical state can be mapped onto an equivalent problem in classical statistics. The path integral formulation of the condensed matter system should first be wick rotated to an Euclidean path integral with imaginary time. This path integral can then be mapped onto the partition sum of a classical system at critical temperature. Then, using classical statistical physics, one can describe the quantum phase transition by a classical thermal phase transition. Since the quantum problem is in such a case equivalent to a statistical problem, the phrase 'stoquastic' is used, referring to both sides of this equivalence: quantum criticality and stochastic. However, as stated, this only works under specific conditions. Due to antisymmetrization for fermions, these conditions are generally not satisfied. This is known as the fermion sign problem. For a review of this problem, the reader is referred to [11] section IV.

Unless the system can be described by a SRE product state (2.8), or can be approached with the stoquastic method, it is beyond polynomial order (it is NP-hard). We have no understanding of how this quantum supreme matter works. One will need a quantum computer to attack this problem. Typical condensed matter systems have a particle number larger than the Avogadro constant $\sim 10^{23-24}$ and quantum computers with similar numbers of qubits are necessary. The current state of the art quantum computers have $\sim 10^2$ qubits and there are promises of $\sim 10^3$ qubits [19]. We are still far from reaching the quantum supremacy necessary to compute these systems of exponential complexity. Another approach is required, and the AdS/CFT correspondence might provide us with one.

Version of June 30, 2022– Created June 30, 2022 - 14:02

Chapter 3

The AdS/CFT Correspondence

The AdS/CFT correspondence offers a new approach for condensed matter physics where the conventional methods fail. Section 3.1 starts off with a short discussion of the holographic principle, which preceded the correspondence. In Section 3.2 the conformal field theory (CFT) side of the correspondence is discussed, followed by Section 3.3 discussing the Anti-de Sitter (AdS) space side. The mathematical machinery to connect both sides of the correspondence is called 'The Dictionary' and is discussed in Section 3.4. In Section 3.5 it is discussed how the correspondence is especially useful for strongly coupled quantum supreme matter; exactly those systems for which conventional condensed matter methods fail. Section 3.6 and Section 3.7 explain how the correspondence is actually a geometrization of the renormalization group flow, and how this viewpoint enables us to make the correspondence more general. Finally in Section 3.8 we discuss how black holes are needed to model the duality of condensed matter systems.

3.1 The Holographic Principle

The AdS/CFT correspondence is preceded by several physical discoveries, motivating and guiding the path towards the formulation of the correspondence. Perhaps the most famous one is the black hole entropy. From thermodynamic considerations, one might expect that the number of micro-states of a system is proportional to the volume of the system, and that therefore the entropy of a black hole grows proportional to its' volume. However the entropy of a black hole scales proportional to its' surface area, as was discovered and formulated by Bekenstein and Hawking [20, 21].

Motivated by the Bekenstein-Hawking entropy and the black hole information paradox, it was found that the maximum amount of information that can be contained in a system is proportional to its surface area. The latter statement, formulated by 't Hooft and Susskind [22, 23], is referred to as the holographic principle: the physical system living in d dimensions is encoded for by the information on its' $(d-1)$-dimensional boundary, just like a hologram is a three-dimensional projection of information on a two-dimensional plate.[1]

[1]The effort of the scientific community is characterized as an ongoing discussion between Leonard

The foremost instance of the holographic principle is the AdS/CFT correspondence, discovered by Maldacena in 1997 [13]. The AdS/CFT correspondence is the conjecture of a duality between a conformal field theory (CFT) and a quantumgravitational theory in an Anti-de Sitter (AdS) space in one dimension higher. To get an understanding of the correspondence, we must first know what a conformal field theory and an AdS space is. The correspondence was originally formulated from a string theory starting point. This is referred to as the top-down approach, as opposed to the bottom-up viewpoint that we take.

3.2 Conformal Field Theory

A conformal field theory is a field theory which enjoys conformal invariance, invariance under conformal transformations. A conformal transformation is an angle-preserving coordinate-transformation:

$$\begin{aligned} x_\mu &\to x'_\mu, \\ g_{\rho\sigma} \to g'_{\rho\sigma}, \quad & g'_{\rho\sigma}\frac{\partial x'^\rho}{\partial x^\mu}\frac{\partial x'^\sigma}{\partial x^\nu} = \Lambda(x) g_{\mu\nu}\,. \end{aligned}$$

This includes translations, rotations (or Lorentz transformations), dilations (scaling transformations) and special conformal transformation.

The behavior of fields under conformal transformations give interesting properties, such as the conformal dimension. This is easiest explained for scalar fields, but can be generalized to other types of fields as well. A field is called a primary field if under a conformal transformation $z \to f(z)$, it transforms as

$$\phi(z) \to \phi'(z) = \left(\frac{\partial f}{\partial z}\right)^\Delta \phi(f(z))\,.$$

It is said to have conformal dimension Δ. Another interesting property which can be derived for conformal field theories is that the energy-momentum tensor is traceless: $T^\mu_\mu = 0$.

Field theories, in $d{+}1$ dimensions, are often described by a Lagrangian. To the Lagrangian of such a theory we can add sources J and their corresponding operators $\mathcal{O}$:

$$\mathcal{L} = \mathcal{L}_{CFT} + \int dx^{d+1} J\mathcal{O}\,.$$

We can now calculate the CFT partition function in terms of the generator functional for the correlation functions as

$$\mathcal{Z}_{CFT} = e^{W(J)} = \left\langle e^{\int dx^{d+1} J\mathcal{O}} \right\rangle_{CFT}\,. \tag{3.1}$$

This object is useful for calculating the n-points functions, which are calculated by taking the n-th functional derivative of $W(J)$ at zero source:

$$\langle \underbrace{\mathcal{O}...\mathcal{O}}_{n} \rangle = \left.\frac{\delta^n W}{\delta J^n}\right|_{J=0}\,. \tag{3.2}$$

Susskind and Stephen Hawking, see the popular science book [24] for an entertaining story and a popular introduction on the topic.

Version of June 30, 2022– Created June 30, 2022 - 14:02

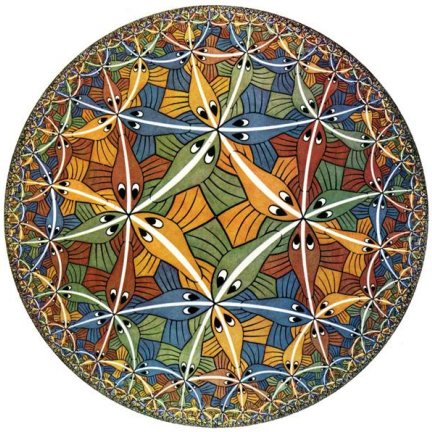

(a) *Circle Limit III by M.C. Escher (1959)*

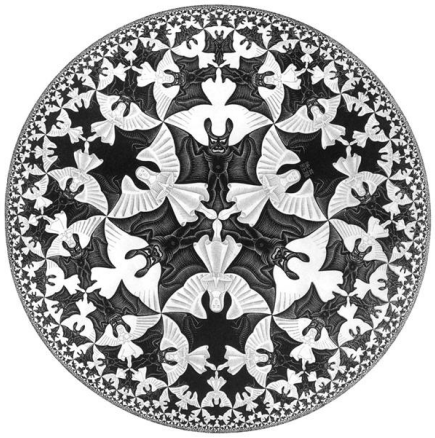

(b) *Circle Limit IV by M.C. Escher (1960)*

Figure 3.1: *Eschers' Circle Limit artworks of hyperbolic planes, representing AdS space.*

3.3 Anti-de Sitter Space-Time

Anti-de Sitter space-time is an exact solution to the Einstein equations for a maximally symmetric empty universe with negative curvature. Similarly the exact solution for positive curvature is the de Sitter space-time and the zero curvature solution is just a Minkowski space-time. It is interesting to note cosmological observations show that our universe has a positive curvature, however we will not use the AdS space-time as cosmological model, but rather as a model for the macroscopic quantum entanglement in metals. The AdS metric is given by

$$ds^2 = \frac{L^2}{z^2}\left(\eta_{\mu\nu}dx^\mu dx^\nu + dz^2\right) , \tag{3.3}$$

where $\eta_{\mu\nu}$ is the Minkowski metric and L is the radius of the AdS space-time. Here z is the radial coordinate such that $z \to 0$ is at spatial infinity, also called the boundary, and $z \to \infty$ is at the center of space. An interesting property of AdS space is that trajectories along null geodesics can reach the boundary in finite time. In this way, the bulk (the centre of the AdS space and the volume around it) and boundary can 'talk' to each other. See Figure 3.1 for a representation of AdS space by the artwork of M.C. Escher.

3.4 The Dictionary

The correspondence is precisely described by what we call the dictionary or the GKPW rule [25, 26]. It states that the partition function of the CFT in $d+1$ dimension is equal to the partition function of the quantum gravitational theory in $d+2$ dimensions evaluated at the boundary ($r \to \infty$), where the boundary field $\phi(x, r \to \infty)$ is equal to the source $J(x)$:

$$\mathcal{Z}_{CFT} = \mathcal{Z}_{\text{grav.}}\big|_{\phi(x,r\to\infty)=J(x)} .$$

We will rename $J(x) \to \phi_0(x)$, such that we can use $\phi(x, r \to \infty) = \phi_0(x)$. The GKPW rule can then be formulated as

$$\left\langle e^{\int dx^{d+1}\phi_0(x)\mathcal{O}(x)}\right\rangle_{CFT} = e^{\mathcal{S}_{\text{bulk}}(\phi(x,r))}\Big|_{\phi(x,r\to\infty)=\phi_0(x)} . \tag{3.4}$$

Version of June 30, 2022– Created June 30, 2022 - 14:02

Dictionary dualities	
Field Theory	Gravitational System
Partition function, $\mathcal{Z}_{\text{field}}$	Partition function, $\mathcal{Z}_{\text{grav.}}$
Stress-energy tensor, $T^{\mu\nu}$	Metric/graviton field, $g_{\mu\nu}$
Current, J^{μ}	Gauge field, A_{μ}
Scalar operator, $\mathcal{O}(x)$	Scalar field, $\phi(x)$
Entropy, s	Area of black hole horizon, A

Table 3.1: *Some dictionary dualities.[27, 28]*

Identifying the field operators with the bulk fields can be done by use of symmetries. One of the characteristics of the duality is that it is a global-local duality: A global symmetry in the field theory corresponds to a gauge symmetry in the bulk. The boundary operator will have the same quantum number as the bulk field, for example a scalar operator corresponds to a scalar field. Many corresponding operators and fields have been identified, for example the metric or graviton field $g_{\mu\nu}$ is dual to the stress-energy tensor $T^{\mu\nu}$ and the $U(1)$ current operator J^{μ} is dual to Maxwell field A_{μ}, see also Table 3.1. A sourced Lagrangian could look like:

$$\mathcal{L} = \mathcal{L}_{CFT} + \int dx^{d+1}\sqrt{g}\left(g_{\mu\nu}T^{\mu\nu} + A_{\mu}J^{\mu} + ...\right) .$$

3.5 The Duality

The power in the use of this duality, for the purposes of this thesis, lies in the fact that the duality is a weak-strong duality. In order to use general relativity instead of a full quantum-gravity, we need weak gravitational coupling. The gravitational coupling constant G corresponds to the planck length $G \sim \ell_p$ up to some constants. The Planck length is the typical length for quantum-gravity fluctuations, and in order to avoid them we require $L \gg \ell_p$. Also to get classical gravity as a limit from the proper top-down approach from string theory, we require a purtubative string theory which is only reliable for small string coupling $L \gg \ell_s$, where ℓ_s is the string length. The dictionary tells us that these limits correspond to $Ng_{CFT} = \lambda \gg 1$ and $N \gg 1$, where N is the number of degrees of freedom in the boundary and g_{CFT} is the CFT coupling constant. λ is called the 't Hooft coupling and is the effective coupling constant for the large N CFT's, characterizing strongly interacting many body entanglement. We thus see that large 't Hooft coupling and the large N limit correspond to classical gravity where the quantum effects can be neglected. There is no need to involve the whole mathematical machinery of string theory and this makes the correspondence extremely powerful for application in condensed matter. Where the conventional condensed matter approach fails, namely for strong interacting many body entanglement, the gravitational theory reduces to it's weakest form: Einstein's general relativity; here we see the essence of the weak-strong duality. In this sense we will try to describe metals with strong correlations by black holes, using classical Einstein gravity and perturbation theory.

Version of June 30, 2022– Created June 30, 2022 - 14:02

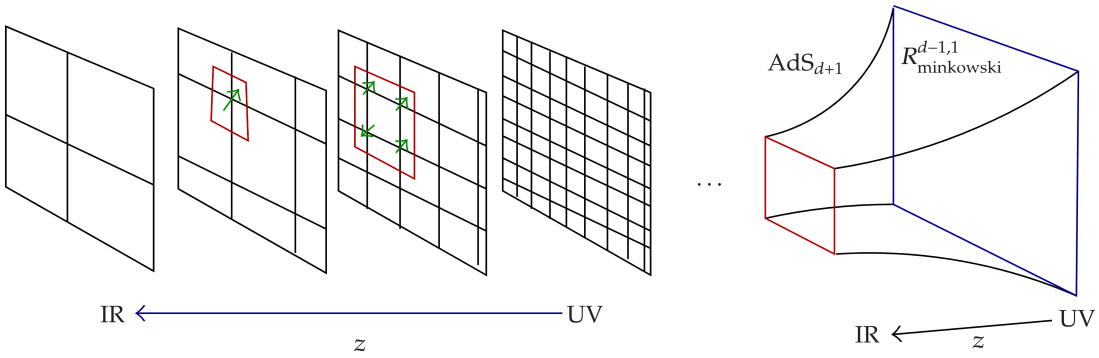

Figure 3.2: *Geometrization of the RG flow. Figure retrieved from [29].*

3.6 Renormalization Group (GR=RG)

From the CFT point of view, we may ask what the physical meaning of this extra radial dimension is. As it turns out, this extra dimensions encodes the RG flow of the system. The renormalization of the energy scale is described by differential equations. These are the beta functions and explain how the coupling constants tranform under scale transformations depending on the energy scale μ,

$$\beta(g,\mu) = \mu \frac{\partial g}{\partial \mu} \,. \tag{3.5}$$

One can put the space-times of the field theory at different μ next to each other in a new dimension, which is parameterized by a coördinate r which is set equal to the energy scale μ. The RG flow is now geometrized in this new extra dimension, see Figure 3.2. This geometrization however depends on two factors. First of all the metric must be invariant under conformal transformations. The second is that under scale transformations $x^\mu \to \lambda x^\mu$, the energy must scale as $r \to \frac{1}{\lambda} r$. This results is the AdS metric:

$$ds^2 = \frac{r^2}{L^2} \eta_{\mu\nu} dx^\mu dx^\nu + \frac{L^2}{r^2} dr^2 \,, \tag{3.6}$$

where r is the radial direction, x^μ the space-time directions orthogonal to r and L is the AdS radius. The boundary lies at $r \to \infty$, and is referred to as the UV, while $r \to 0$ is referred to as the IR. In other words, the deep interior of the AdS space encodes the macroscopic scales of the field theory. A reparametrization $z = \frac{L^2}{r}$ gives us

$$ds^2 = \frac{L^2}{z^2} \left(\eta_{\mu\nu} dx^\mu dx^\nu + dz^2 \right) \,, \tag{3.7}$$

where now $z \to 0$ denotes the boundary and the UV, while $z \to \infty$ is the IR. This is exactly (3.3). We thus see that general relativity (GR) is a geometrization of the renormalization group (RG) flow, which can be summarized in the "equation": GR=RG (note that in the rest of this thesis GR will be the abbreviation for 'Gubser-Rocha').

The concept of the RG flow is that physical systems depend locally on the energy scale μ. By course graining, we integrate out the high energy UV physics, which is irrelevant at the IR low energies. As can be seen from (3.5), a fixed point in the RG flow corresponds to $\beta(g,\mu) = 0$. At a fixed point, the system does not depend on the energy scale anymore

Version of June 30, 2022– Created June 30, 2022 - 14:02

and scale invariance is implied. By introducing operators in our theory, we can deform the scale (or conformal) invariance and thereby alter the RG flow. Depending on the conformal dimension Δ, the RG flow might flow away from a UV fixed point towards a IR fixed point, meaning that the IR is independent of the UV. This independence of the high energy details can then be recognized as universality.

3.7 Gauge/Gravity duality

Although CFT's are powerful to describe systems with scale invariance, for application in condensed matter one requires finite temperature and finite density, which introduce energy scales, breaking the conformal symmetry. With the intuition of the geometrization of the RG flow, we can understand that by altering the boundary we get a different RG flow resulting in a different the bulk geometry. This generalization of the correspondence can be called the Gauge/Gravity duality. We can still use the dictionary since the gravitational problem only needs to be asymptotically AdS in the boundary/UV. For this reason we can have a more general gravitational system than pure AdS, for example black holes in an AdS background. Adding a black hole in the AdS bulk gives rise to a black hole temperature and entropy, which dualizes to finite temperature in the boundary. Following the duality between the 4-current in the boundary and the Maxwell field in the bulk, we find that by giving the black hole a charge, we get a finite density system in the boundary.

3.8 Black Holes

So the idea is to put a charged black hole in the bulk, such that the boundary field theory describes finite density and finite temperature. A solution to the Einstein-Maxwell equation is the Reissner-Nordström (RN) black hole. It has a finite mass, finite charge and has two horizons. This black hole can achieve both finite temperature and finite density. In an extremal RN black hole the two horizons coincide and the surface gravity vanishes. The result is that the horizon with a finite area has no Hawking radiation and therefore no temperature. This black hole describes a metal with zero temperature entropy, which is thermodynamically not allowed. This can be solved by adding a dilaton field, these types of fields are very common in string theory. From the top-down approach of string theory one never acquires a RN black hole in $3+1$ space-time dimensions. String theory is formulated in more space-time dimensions and one has to 'roll up' or compactify those extra dimensions. The result of the compactification is that there is an additional dilaton field. In the resulting Einstein-Maxwell-Dilaton (EMD) theory, the zero temperature entropy is avoided. This will be the theory used in this thesis. The EMD background black hole solution, provided by Gubser and Rocha [30] will be used (see Section 5.1.2).

Chapter 4

Condensed Matter Theory for Holographic Strange Metals

This chapter aims to provide a better understanding of the strange metal and how holography will offer a better understanding of these metals. Section 4.1 discusses local quantum criticality in strange metals. It discusses a general metric useful to describe a general class of metals including the quantum critical ones. To be able to talk about transport properties, one needs a mechanism to dissipate momentum. Section 4.2 explains how a lattice will do this. Then Section 4.3 and Section 4.4 discuss some important properties that govern the holographic metals and account for the behavior in quantum supreme matter. In Section 4.5 it is explained that these results are only valid within a certain regime and that the transport properties scale differently outside this regime. Limits on these holographic properties may cause a saturation in the length over which the momentum can dissipate as discussed in Section 4.6. The chapter is concluded with Section 4.7 providing equations for the transport coefficients.

4.1 Local Quantum Criticality

In statistical physics, we can describe the transition between two phases of a system with a phase transition. The transition is controlled by some parameter, for example the temperature. Below some critical temperature T_C the system is in an ordered state, while above T_C the system is in the disordered state. Thermodynamic properties in continuous phase transitions turn out to be described by power-laws, characterized by critical exponents. From renormalization group theory, one finds that the phase transition typically does not depend on UV properties, but on properties such as dimension and symmetry. As a result, the critical exponents will be the same for a range of systems with different microscopic physics, but with same dimension and symmetries. We say that the critical exponents are universal. The phenomenon of universality is that certain parameters can be the same for many different physical systems, independent of their microscopic properties. This independence of the UV can be recognized when looking at the correlation length. The power-law of the correlation length shows divergence at the critical point, introducing scale invariance and independence of microscopic details. Other than a thermal

phase transition, one can also have Quantum phase transitions. These happen at zero temperature, since only at extremely low temperature the quantum fluctuations will take over from the thermal fluctuations controlling the transition. The control parameter will then often be the magnetic field, pressure or even doping. The peculiarity of the quantum critical point is that the physics of the system knows about the quantum critical point, also further away from the quantum critical point. The result is the famous quantum critical wedge, for which we refer back to Figure 1.2. At the quantum critical point one typically not only has scale- but even conformal invariance. Metals may experience a continuous quantum phase transition to a phase of non-Fermi liquid behavior: the strange metal phase. Due to the conformal symmetry of the quantum critical point, CFT's are an excellent way to describe these systems. This way the AdS/CFT correspondence may help us to learn about the strange metal phase.

Taking a look back at the stoquastic approach, one used the Euclidean signature where space and time are on the same footing. Here we had the AdS_{d+2} metric (3.6)

$$ds^2 = -r^2 dt^2 + r^2 \sum_{i=1}^{d} dx_i^2 + \frac{dr^2}{r^2}\,, \tag{4.1}$$

where we chose $L = 1$. This has Lorentzian scaling

$$t \to \lambda t\,, \quad x_i \to \lambda x_i\,, \quad r \to \lambda^{-1} r\,, \quad ds \to ds\,. \tag{4.2}$$

However with the stoquastic approach one can get an action in which the time direction is not equivalent to a space direction. This is captured by including the *dynamical scaling exponent* z:

$$ds^2 = -r^{2z} dt^2 + r^2 \sum_{i=1}^{d} dx_i^2 + \frac{dr^2}{r^2}\,, \tag{4.3}$$

which results in Lifshitz scaling

$$t \to \lambda^z t\,, \quad x_i \to \lambda x_i\,, \quad r \to \lambda^{-1} r\,, \quad ds \to ds\,, \tag{4.4}$$

where we see how time scales with respect to space. For $z = 1$ one recovers the isotropic Euclidean space-time, corresponding to Lorentz invariance. However for other values of z, one gets z time dimensions in their Euclidean space-time. for $z \to \infty$ space does not scale, only time does. Therefore we refer to this as local quantum criticality [11]. In the cuprate strange metals, quantum criticality and thus $z \to \infty$ is realized [31, 32]. We can also violate the scale invariance of the metric by including the *hyperscaling violation exponent* θ [33, 34]. The background metric will look like

$$ds^2 = r^{-2\frac{\theta}{d}} \left(-r^{2z} dt^2 + r^2 \sum_{i=1}^{d} dx_i^2 + \frac{dr^2}{r^2} \right)\,, \tag{4.5}$$

where the scaling is now of the form

$$t \to \lambda^z t\,, \quad x_i \to \lambda x_i\,, \quad r \to \lambda^{-1} r\,, \quad ds \to \lambda^{\frac{\theta}{d}} ds\,. \tag{4.6}$$

For $\theta = 0$ hyperscaling is recovered. Only for $z = 1, \theta = 0$ relativistic conformal invariance is restored. Of course as we alter the bulk geometry, the physics in the boundary should be altered accordingly. We now find that the entropy scales with the temperature as [35]

$$s \sim T^{\frac{d-\theta}{z}} . \tag{4.7}$$

The hyperscaling exponent θ turns out to describe the number of relevant thermodynamic degrees of freedom [11]. For the $z = 1$ Fermi-liquid this is equal to the dimensionality of the Fermi surface in momentum space which is $\theta = d-1$. We therefore recover the typical Sommerfeld entropy $s \sim T$ for the Fermi liquid. The strange metal is also observed to have a Sommerfeld entropy, but local quantum critical systems have $z \to \infty$ which seems to imply a zero temperature entropy, which we know exists in the RN holographic metal. However the proper string theoretical computation of the EMD theory [30] will provide us with $z \to \infty, \theta \to -\infty$, such that $\eta = \frac{-\theta}{z} = 1$, resulting in $s \sim T$. This means that the strange metal cannot be described by a $\theta = d - 1$ dimensional Fermi surface.

4.2 Breaking Translation Invariance

In the homogeneous background, the system enjoys translation invariance. Translation invariance implies conservation of momentum. As discussed in Chapter 2, in order to describe physical metals, we wish to dissipate momentum. The starting point of many descriptions of metals is the crystal structure of the system. A crystal structure results in umklapp scattering. In umklapp scattering, only crystal momentum is conserved. The consequence is the Brillouin zones in phase space. Due to the periodicity of the crystal, all momentum wavevectors outside the first Brillouin zone can equivalently be described by a wavevector inside the first Brillouin zone. In the spectrum for the one-dimensional lattice, this can be seen as the dispersion folding into the first Brillouin zone, this can be seen as a turning over ('umklapp') of the dispersion at the boundary of the Brillouin zone. The system can now dissipate momentum via this umklapp mechanism. This is the way we will also break translation invariance in the holographic setup. We will explicitly introduce a periodic potential in the boundary, see Section 5.2. In the unparticle system there are no quasiparticle decay rates, only the momentum decay. Therefore the resistivity of the metal is governed by the momentum dissipation due to the lattice.

4.3 Planckian Dissipation and Minimal Viscosity

Measurements have shown that the relaxation times in strange metals is of the order of the Planckian time $\tau_k \sim \tau_\hbar = \frac{\hbar}{k_B T}$. This time is the most fundamental time associated with temperature one can come up with in physics from just dimensional analysis. The dissipation set by this timescale is 'Planckian dissipation' [36]. It is the fastest rate at which momentum can dissipate and entropy can be produced. This is a result of the *eigenstate thermalization hypothesis*, which explains why quantum systems may be described by stochastics. For an N particle system, unitary time evolution keeps track of 2^N bits. No entropy is produced during the unitary time evolution, but by making observations, the wave function collapses, information is lost and entropy is produced. From our classical observational viewpoint we can only observe N bits, and if the time

Version of June 30, 2022– Created June 30, 2022 - 14:02

evolution is sufficiently long we will always observe an equilibrium state with an associated temperature T. The more entangled the system is, the more entropy will be produced upon collapsing the wave function. From the stoquastic approach this is easily understood. For the scale invariant quantum critical system, the Euclidean time is a circle with radius $\frac{\hbar}{k_B T}$. This is the only scale in the otherwise scale invariant system, which becomes the dissipation time scale when we go back to Lorentzian time. We can compare this with the Fermi Liquid where there is another time scale: the Fermi energy. The momentum relaxation time is set by the collision time which is the Planckian time altered by a factor associated with the Fermi energy scale $\tau_c \sim \frac{E_F}{k_B T}\tau_\hbar$. The Planckian time scale is conjectured to be the shortest time for momentum relaxation [36], and we expect that this minimum is reached only for very strongly interacting metals.

Finite temperature holography tells us that the CFT side is described by relativistic hydrodynamics, where dissipation is governed by the shear viscosity [37]. The viscosity turns out to be proportional to the area of the Schwarzschild black hole, which also sets the entropy. The result is a very small viscosity given by

$$\frac{\eta}{s} = \frac{1}{4\pi}\frac{\hbar}{k_B}\,. \tag{4.8}$$

This is believed to be a lower bound on the viscosity, also for systems that do not have a gravitational dual [38]. The minimal viscosity can actually be regarded as a manifestation of the Planckian dissipation. We will approach this with dimensional analysis. The hydrodynamic viscosity is given by the free energy f and momentum relaxation time: $\eta \sim f\tau_K$. Due to the absence of energy scale, the scale invariant system has a free energy set by the entropy $f = sT$. Now the Planckian dissipation kicks in, the momentum relaxation is set by the only relaxation time in the system $\tau_K = \tau_\hbar$. Plugging everything in we find the minimal viscosity $\eta \sim sT\tau_\hbar = s\frac{\hbar}{k_B}$. The minimal viscosity is found to be obeyed in the quark-gluon plasma [39].

4.4 Linear in T Resistivity.

Due to the *unparticle* physics, we must work with the collective physical transport properties instead of those of individual quasiparticles. Therefore we will consider the total current and total momentum. Note that Drude theory, although easily explained in the context of particles, does not require particles. Only a way of momentum dissipation is necessary and Drude theory can still be applied.

Strange metals have been experimentally observed to have a linear in temperature resistivity [40]. An explanation was discovered by Davison, Schalm and Zaanen [41]. An universal mechanism is shown to result in a linear resistivity, for systems that can be described by hydrodynamics in the IR and that have a minimal viscosity, which are the properties of our strange metal description. They show that the resistivity will have a viscous contribution which is proportional to the entropy. The formal discovery comes from memory matrix calculations, of which the details will remain outside of the scope of this thesis. But arguments can be made with some simple physical reasoning [18]. We depart from a hydrodynamical fluid with minimal viscosity and local quantum criticality. In a system with broken translation invariance, the momentum dissipation rate $\Gamma = \tau_K^{-1}$

is characterized by a diffusivity constant and the length scale of the broken translation invariance ℓ_η characterizing the shear drag length as

$$\Gamma = \frac{\mathcal{D}}{\ell_\eta^2}\,. \tag{4.9}$$

In a relativistic hydrodynamical fluid, the diffusion constant is $\mathcal{D} = \frac{\eta}{\mathcal{E}+\mathcal{P}}$, where η is the viscosity and $\mathcal{E}$ and $\mathcal{P}$ are the energy and pressure. For a non-relativistic fluid this becomes $\frac{\eta}{mn}$, where m is the electron mass and n the number density. Now since our system is strongly interacting, it has a minimal viscosity (4.8). Using $\frac{\eta}{s} = A_\eta \frac{\hbar}{k_B}$ to allow for slightly different proportionality factors (still of order unity) this results in

$$\Gamma = \frac{\hbar}{k_B}\frac{A_\eta\, s}{(\mathcal{E}+\mathcal{P})\ell_\eta^2}\,, \tag{4.10}$$

where we now see that the momentum relaxation rate is proportional to the entropy. Drude theory tells us that the DC resistivity is given by (2.5),

$$\rho = \frac{1}{\omega_p^2}\Gamma\,. \tag{4.11}$$

At low temperatures ω_p should be independent of temperature. The whole temperature dependence of the resistivity is therefore set by the temperature dependence of momentum relaxation rate. We can thus conclude that the resistivity should be proportional to the entropy. So therefore, in system with Sommerfeld entropy $S \sim T$, the resistivity is indeed proportional to the temperature.

4.5 Outside the Hydrodynamical Regime

Hydrodynamics is the effective description of a system at long times and distances, where the dynamics are dominated by the long-lived modes and one can ignore the microscopic details. In the previous sections we used the hydrodynamic description of our metal, but this does not hold when we go to smaller length scales. The difference between these regimes has been studied by Iqbal, Liu and Mezei [42]. They show that for length scales larger than a correlation length $\xi_\mu = \frac{\pi}{\sqrt{2}}\mu^{-1}$, the correlations decay exponential. The results of this is that the system consists of patches of the size of the correlation length which are only weakly correlated. These patches do not have causal contact in the bulk, resulting in uncorrelated domains in the boundary. From a macroscopic view we can then apply hydrodynamics. However, within such a domain the correlations are governed by power-laws.

The scaling of the conductivity in the holographic metal in this regime can be described. For the RN metal this was done by Hartnoll and Hofman [43]. However Anantua et al. [44] consider a more general case for $0 < \eta < 2$, where η is a scaling exponent defined by $s \propto T^\eta$ (for RN $\eta = 0$ due to the zero temperature entropy and $\eta = 1$ for the EMD metal). The longitudal conductivity of the system is expressed in terms of the retarded Green's funcion of the charge,

$$\sigma(k) = \lim_{\omega\to 0}\frac{\operatorname{Im} G^R_{J^tJ^t}(\omega,k)}{\omega}\,. \tag{4.12}$$

Doing the calculations, Anantua et al. show that for the longitudonal conductivity and weak lattices one gets

$$\begin{aligned}\sigma &\propto T^{2\nu-1}\,,\\ \nu &= \frac{1+\eta}{2\sqrt{2+\eta}}\sqrt{10+\eta+4(2+\eta)\,(k)^2-8\sqrt{1+(2+\eta)\,(k)^2}}\,.\end{aligned} \tag{4.13}$$

This scaling of the conductivity outside the hydrodynamic regime can be checked. This means that outside the hydro regime $\ell_\eta < \xi = \frac{\pi}{\sqrt{2}}\mu^{-1}$ or $G > \frac{\sqrt{2}}{\pi}\mu$, (4.13) can be fit to the data of weak lattices.

4.6 Shear Length

The correlation length can be regarded as the shortest length over which the metal experiences shear drag. On smaller scales a different regime is entered, where there is no shear drag. By making the influence of the lattice stronger, one would expect the length scale of the shear drag to reach this minimum. putting $\ell_\eta = \xi_\mu$. From (4.10) and (4.11), we can conclude that this bounds the resistivity. Increasing the strength of the lattice one could expect a saturation for the resistivity.

4.7 Transport Coefficients

Using relativistic hydrodynamics and the memory matrix formalism, one can find expressions for the optical conductivities [45, 46]

$$\begin{aligned}\sigma &= \frac{n^2}{\mathcal{E}+\mathcal{P}}\frac{1}{\Gamma-i\omega}+\sigma_Q\,,\\ \alpha &= \frac{ns}{\mathcal{E}+\mathcal{P}}\frac{1}{\Gamma-i\omega}+\alpha_Q\,,\\ \frac{\bar\kappa}{T} &= \frac{s^2}{\mathcal{E}+\mathcal{P}}\frac{1}{\Gamma-i\omega}+\frac{\bar\kappa_Q}{T}\,,\end{aligned} \tag{4.14}$$

where all the first terms are of the Drude form, arising from momentum relaxation. Note that these all differ by the ratio of charge density over entropy density like $\sigma_{Drude} = \frac{n}{s}\alpha_{Drude} = \frac{n^2}{s^2}\frac{\bar\kappa_{Drude}}{T}$. The second terms will be referred to as the incoherent conductivities[1], accounting for charge transport which is decoupled from the total momentum. For Galilean invariance, it can be shown that $\sigma_Q = \alpha_Q = \bar\kappa_Q = 0$. However for the relativistic case, the incoherent contributions can be finite. When translation symmetry is broken, heat and charge transport may couple and the incoherent contributions will be related as

$$\begin{aligned}\sigma &= \frac{n^2}{\mathcal{E}+\mathcal{P}}\frac{1}{\Gamma-i\omega}+\sigma_Q\,,\\ \alpha &= \frac{ns}{\mathcal{E}+\mathcal{P}}\frac{1}{\Gamma-i\omega}-\frac{\mu}{T}\sigma_Q\,,\\ \frac{\bar\kappa}{T} &= \frac{s^2}{\mathcal{E}+\mathcal{P}}\frac{1}{\Gamma-i\omega}+\frac{\mu^2}{T^2}\sigma_Q\,.\end{aligned} \tag{4.15}$$

[1] As one might not associate coherence with transport properties, this naming is not the most intuitive. However it comes for the fact that for particles an experimentalist will find coherent excitation in their spectrum.

Version of June 30, 2022– Created June 30, 2022 - 14:02

However Davison and Goutéraux [47] tell us that that calculation was incomplete, and that the proper equations should be

$$\begin{aligned}
\sigma &= \frac{\frac{n^2}{\epsilon+p} + \Gamma\left(1-\sigma_Q+\lambda\mu^2\right) + O\left(\Gamma^2,\omega\Gamma,\omega^2\right)}{\Gamma - i\omega} + \sigma_Q + O(\omega,\Gamma)\,, \\
\alpha &= \frac{\frac{ns}{\epsilon+p} + \Gamma\left(\frac{\mu}{T}\sigma_Q + 4\pi n\lambda\right) + O\left(\Gamma^2,\omega\Gamma,\omega^2\right)}{\Gamma - i\omega} - \frac{\mu}{T}\sigma_Q + O(\omega,\Gamma)\,, \\
\frac{\bar{\kappa}}{T} &= \frac{\frac{s^2}{\epsilon+p} + \Gamma\left(-\frac{\mu^2}{T^2}\sigma_Q + 4\pi s\lambda\right) + O\left(\Gamma^2,\omega\Gamma,\omega^2\right)}{\Gamma - i\omega} + \frac{\mu^2}{T^2}\sigma_Q + O(\omega,\Gamma)\,,
\end{aligned} \tag{4.16}$$

where λ is a function depending only of T and μ. To first order in Γ and ω the DC incoherent contributions cannot be distinguished from the coherent part.

Chapter 5

The Setup

In this chapter we will first explain the black holes used for the computation in Section 5.1. Next in Section 5.2 we will explain how an explicit lattice is introduced to break translation symmetry and allow for momentum dissipation. Finally in Section 5.3 we shortly discuss the numerical computations.

5.1 Black Holes in AdS space

5.1.1 Reissner-Nordström Black Hole

Condsider the AdS Einstein-Maxwell action:

$$S = \int dx^{d+1}\sqrt{-g}\left(R - 2\Lambda - \frac{1}{4}F_{\mu\nu}F^{\mu\nu}\right) \tag{5.1}$$

where $2\Lambda = -\frac{(d-1)(d)}{L^2}$. We chose units such that $c = e = 1$ and $16\pi G = 1$.
Consider the Einstein-Maxwell field equations

$$\begin{aligned} &\nabla_\mu F^{\mu\nu} = 0 \\ &R_{\mu\nu} - \frac{1}{2}Rg_{\mu\nu} + \Lambda g_{\mu\nu} = \frac{1}{2}T_{\mu\nu}\,, \\ &T_{\mu\nu} = F_{\mu\rho}F_\nu{}^\rho - \frac{1}{4}g_{\mu\nu}F_{\rho\sigma}F^{\rho\sigma}\,. \end{aligned} \tag{5.2}$$

A static solution to the Einstein-Maxwell equations is the Reissner-Nordström metric:

$$\begin{aligned} ds^2 &= -\frac{r^2}{L^2}\left(-f(r)dt^2 + d\mathbf{x}^2\right) + \frac{L^2}{r^2}\frac{dr^2}{f(r)} = \frac{L^2}{z^2}\left(-\tilde{f}(z)dt^2 + \frac{dz^2}{\tilde{f}(z)} + d\mathbf{x}^2\right)\,, \\ f(r) &= 1 + \frac{Q^2}{r^{2(d-1)}} - \frac{M}{r^d}\,, \quad \tilde{f}(z) = f(r = L^2/z)\,, \\ A_t(r) &= \mu(1 - \frac{r_0^{d-2}}{r^{d-2}}) = \mu(1 - \frac{z^{d-2}}{z_0^{d-2}})\,, \end{aligned} \tag{5.3}$$

where M, Q are (proportional to) the total mass and total charge of the black hole and r_0, z_0 is the position of the outer horizon. These black holes have two horizons and by looking

at the Penrose diagrams we can connect infinitely many maximally extended RN metrics. For the case that the horizons "overlap" we speak of an extremal RN black hole. However as noted in Section 3.8, the RN black hole gives a zero temperature entropy, so cannot give an accurate description of a real physical system and is only phenomenological. The holographic metal of the RN black hole is discussed in the theses [14, 15]. We will use some data of this black hole as comparison to our Gubser-Rocha metal.

5.1.2 Gubser-Rocha Black Hole

As discussed, from string theory one always end up with a dilaton field after compatifying the 'extra' dimensions, which will fix the zero temperature entropy problem. Starting out with Einstein-Maxwell-Dilaton theory (EMD), we will consider the following action: [30, 48]

$$S_{EMD} = \frac{1}{2\kappa^2}\int d^2\sqrt{-g}\left(R - \frac{e^{\phi}}{4}F_{\mu\nu}F^{\mu\nu} - \frac{3}{2}\left(\partial_\mu\phi\right)^2 + V(\phi)\right), \tag{5.4}$$

where $V(\phi) = \frac{6}{L^2}\cosh\phi$ and we will set $2\kappa^2 = L^2 = 1$. An analytical solution to the resulting equations is

$$\begin{aligned} ds^2 &= \frac{L^2}{z^2}\left(-f(z)dt^2 + \frac{dz^2}{f(z)} + g(z)\left(dx^2+dy^2\right)\right), \\ A_t(z) &= L\sqrt{3Q}(1-z)\frac{\sqrt{1+Q}}{1+Qz}, \\ \phi(z) &= \frac{1}{2}\ln(1+Qz), \\ f(z) &= (1-z)\frac{p(z)}{g(z)}, \quad g(z) = (1+Qz)^{3/2}, \\ p(z) &= 1+(1+3Q)z+(1+3Q(1+Q))z^2. \end{aligned} \tag{5.5}$$

Where z is the same radial coordinate as used before. The horizon is located at $z = 0$ and due to choice of constants, the black hole horizon is now located at $z = 1$. We will refer to this black hole as the Gubser-Rocha (GR) black hole. This is the black hole that will be used to produce our data.

5.2 Breaking Translations

Momentum conservation is associated with translation symmetry. To introduce momentum relaxation explicitly, we need to break translation invariance. Just like in real metal the translation symmetry is broken by a lattice, we will introduce a periodic ionic lattice potential in the boundary

$$A_t(z=0) = \bar{\mu}\left(1 + A_1\cos\left(G_x x\right) + A_2\cos\left(G_y y\right)\right) \tag{5.6}$$

The resulting equations of motions will be complicated non-linear PDE's. To solve these, computational power is needed.

5.3 Computation

The computations are made by a numerical code written by F. Balm [49]. Large computational power is needed, so the code is run on supercomputers. The supercomputer ALICE in Leiden and Snellius in Amsterdam have been used to perform the numerics. The code makes use of finite difference methods to solve the differential equations. For the RN geometry, an equidistant spacing in the radial direction was used. However this same spacing did not perform well for the more complicated GR geometry resulting in numerical issues. To solve this a Chebyshev spacing was used. This has a more dense spacing near the horizon and the boundary and a less dense spacing in between. This should give better results since the numerical accuracy failed near the horizon and the boundary. Needing even more accuracy to get physical acceptable thermodynamic quantities, the density of the Chebyshev spacing was cubed, making the spacing near the horizon and boundary even more dense.

Version of June 30, 2022– Created June 30, 2022 - 14:02

Chapter 6

Results

For the presented results, natural units are chosen and all quantities are presented in dimensionless units. The temperature is in units of μ, the entropy and the density are in units of μ^2, while the energy and pressure are in units of μ^3.

First in Section 6.1 the underlying thermodynamics will be presented. In Section 6.2 the linear in T resistivity is presented along with all the thermo-electric conductivities. Section 6.3 shows the crossover from the hydro regime to the power-law scaling regime, and also fits the scaling of the electric conductivity.

6.1 Thermodynamics

The thermodynamic quantities can be calculated from the bulk and some are presented in Figure 6.1. Firstly we notice that the ratio of energy over pressure is $\frac{\mathcal{E}}{\mathcal{P}} = 2$ for all lattice strengths. Since the pressure in the x and y direction are the same $\mathcal{P}_x = \mathcal{P}_y = \mathcal{P}$, this means that the trace of the stress energy tensor indeed vanishes. This should hold for conformal invariance. We see that this also holds when the translations are broken by a lattice. Next we notice that the first law of thermodynamics seems to hold for weak lattices. The first law of thermodynamics is given by

$$\mathcal{E} + \mathcal{P} = Ts + \mu n\,, \tag{6.1}$$

is obeyed as the homogeneous limit is approached. In the figure, the ratio of the r.h.s and the l.h.s of (6.1) is plotted, which approaches unity for weaker lattices. However one might expect a larger deviation based on recent research, see Chapter 7 for a discussion. The figure also clearly shows a Sommerfeld entropy $s \sim T$. And finally the ratio $\frac{s}{n}$ is included, since this is the proportionality factor relating the different Drude conductivities.

6.2 Transport

In the boundary the conductivities have been computed and the results are presented in Figure 6.2 and Figure 6.3. In Figure 6.2 one can observe the famous linear in temperature resistivity. In Figure 6.3 we see how the different conductivities scale with temperature.

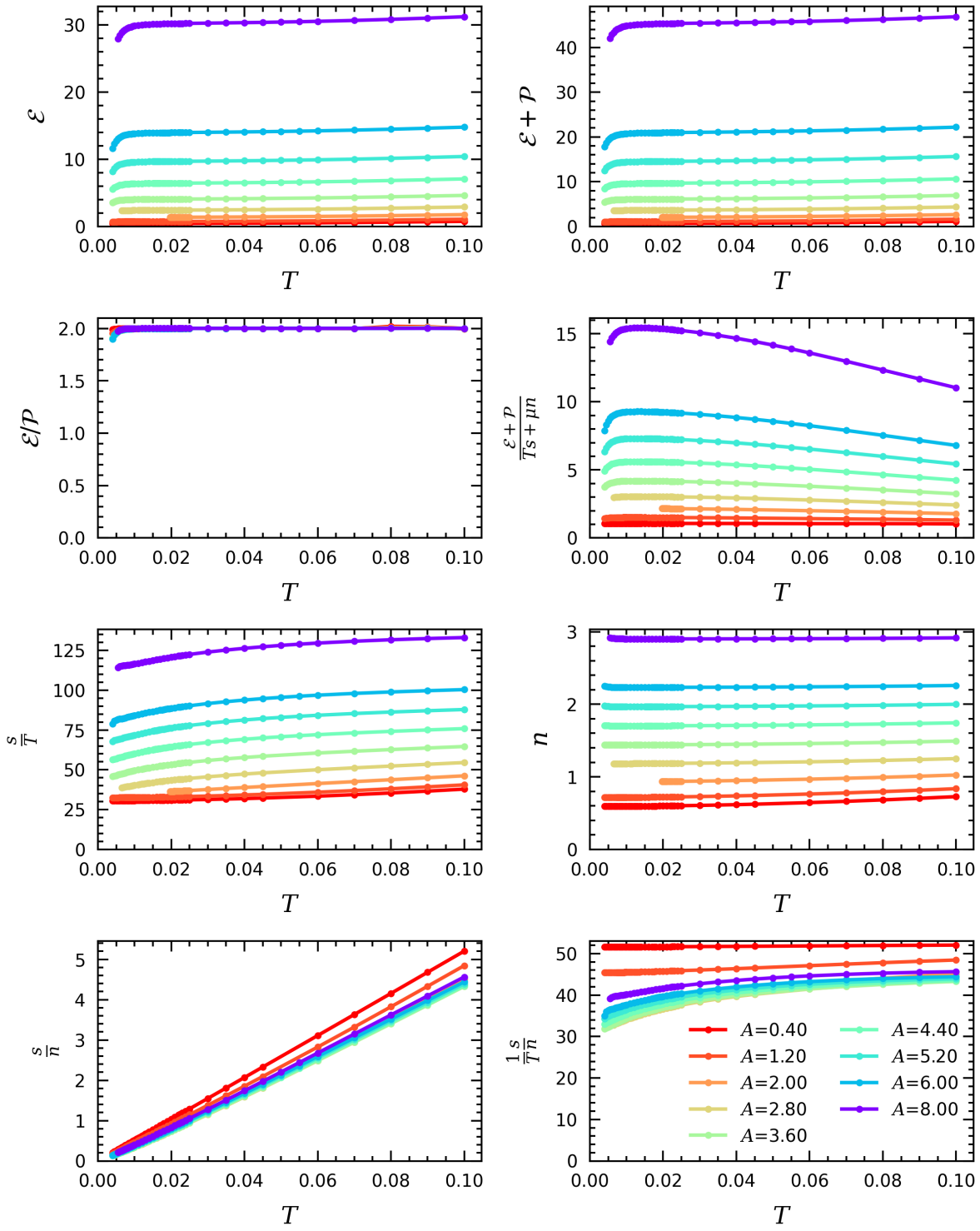

Figure 6.1: *Results of the thermodynamics of the Gubser-Rocha metal. See Section 6.1.*

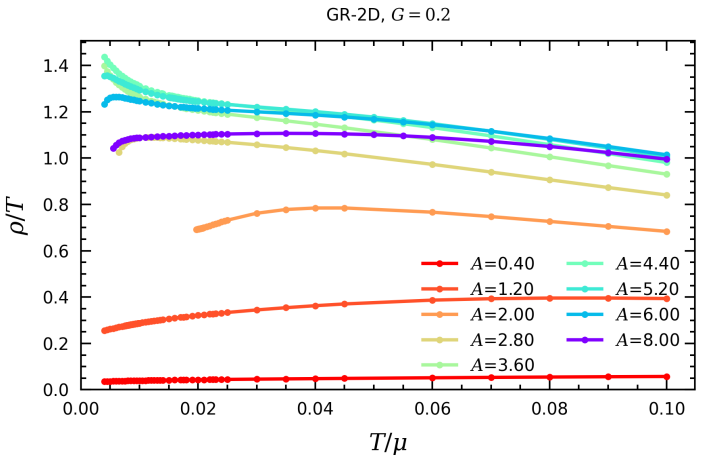

Figure 6.2: *The Gubser-Rocha metal reproduces the famous linear in temperature resistivity.*

The left column is the Gubser-Rocha metal, while the right column is the Reissner-Nordström metal, which is included for comparison. Due to the linear in T resistivity, the electric conductivity is plotted as σT for Gubser-Rocha, while for RN just as σ due to the zero-temperature entropy. Since s is linear in T for GR and all Drude conductivities differ a factor $\frac{s}{n}$ which is also linear in T as seen in Figure 6.1, we multiple each lower panel the conductivity with an extra factor $\frac{1}{T}$ for visualization of the scaling behavior. For RN there is of course the zero-temperature entropy, so this column does not get additional temperature dependent factors. Furthermore, as the lattice strength A increases, the conductivities seem to saturate. From these conductivities, one can calculate $\sigma_{Q=0}$ and κ by (2.2) and (2.3). This transport coefficients characterizing the transport for decoupled heat and momentum are depicted in figure Figure 6.4.In the homogeneous case these are very small, but for increasing lattice strength they reach significant values, which can be seen when comparing their values to Figure 6.3.

6.3 Outside the Hydrodynamic Regime

As discussed in Section 4.5, the resistivity has different scaling regimes depending on the lattice vector G. To visualize this, the a log-log plot of the resistivity against temperature is shown in Figure 6.5 for different values of G. For small G or large distances we are still in the hydro regime. While the $G = 0.4\mu$ data seems to be in the hydro regime, the $G = 0.6$ clearly shows power-law behavior. However the strong lattice (A=4) loses this power-law behavior. This is consistent with the prediction from Section 4.5 that for $G > \frac{\sqrt{2}}{\pi}\mu \approx 0.45\mu$ the resistivity scales as power-laws for weak lattice strength. The power-law scaling according to (4.13) is fitted in Figure 6.6. The blue dashed line is the prediction by (4.13), while the red dots are the fitted data point. A good match is observed for weak lattices.

Version of June 30, 2022– Created June 30, 2022 - 14:02

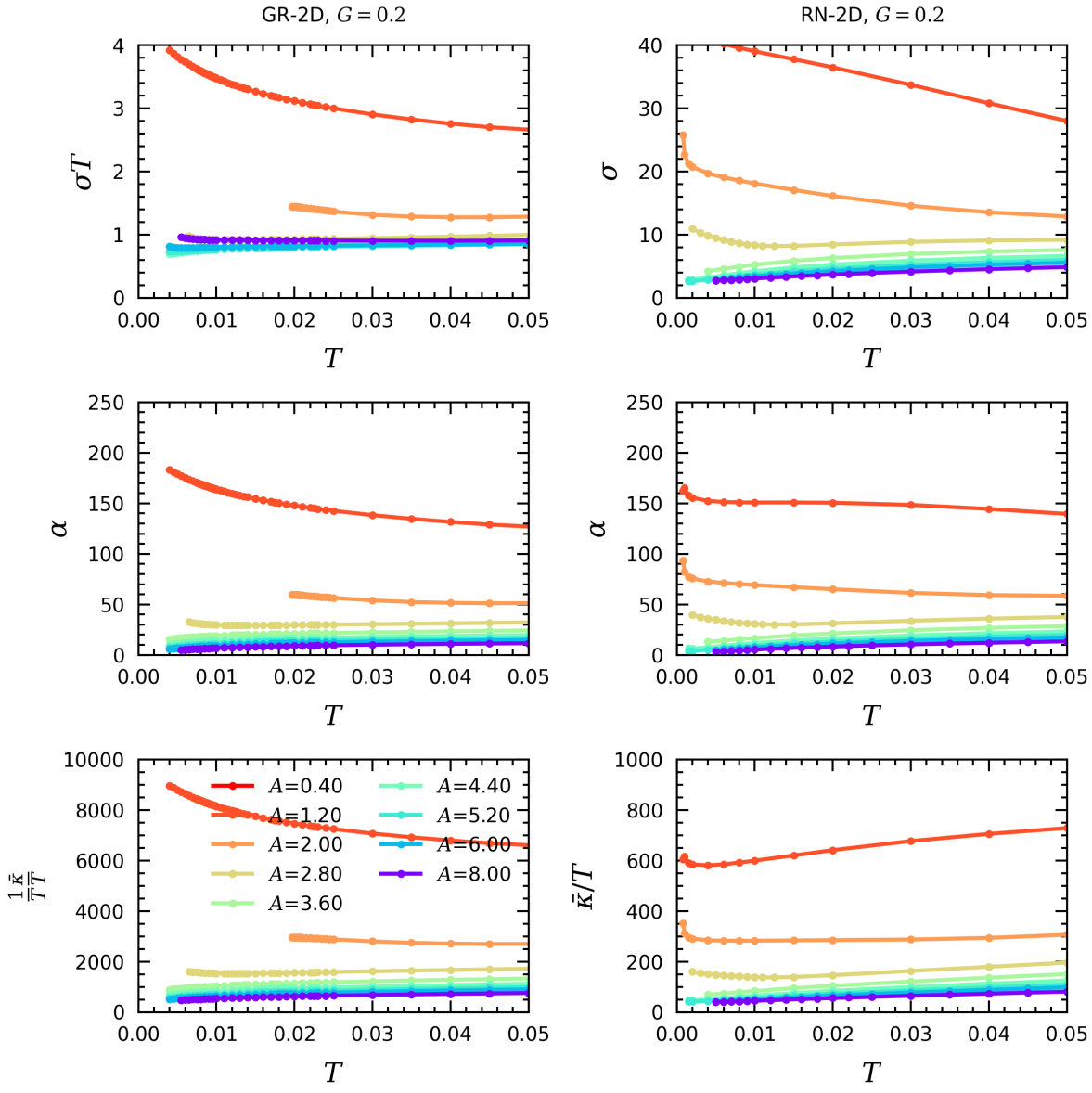

Figure 6.3: *The scaling in T/μ of the different thermo and electric conductivities. Left is for the Gubser-Rocha (GR) metal and for comparison the Reissner-Nordström (RN) metal data is included on the right.*

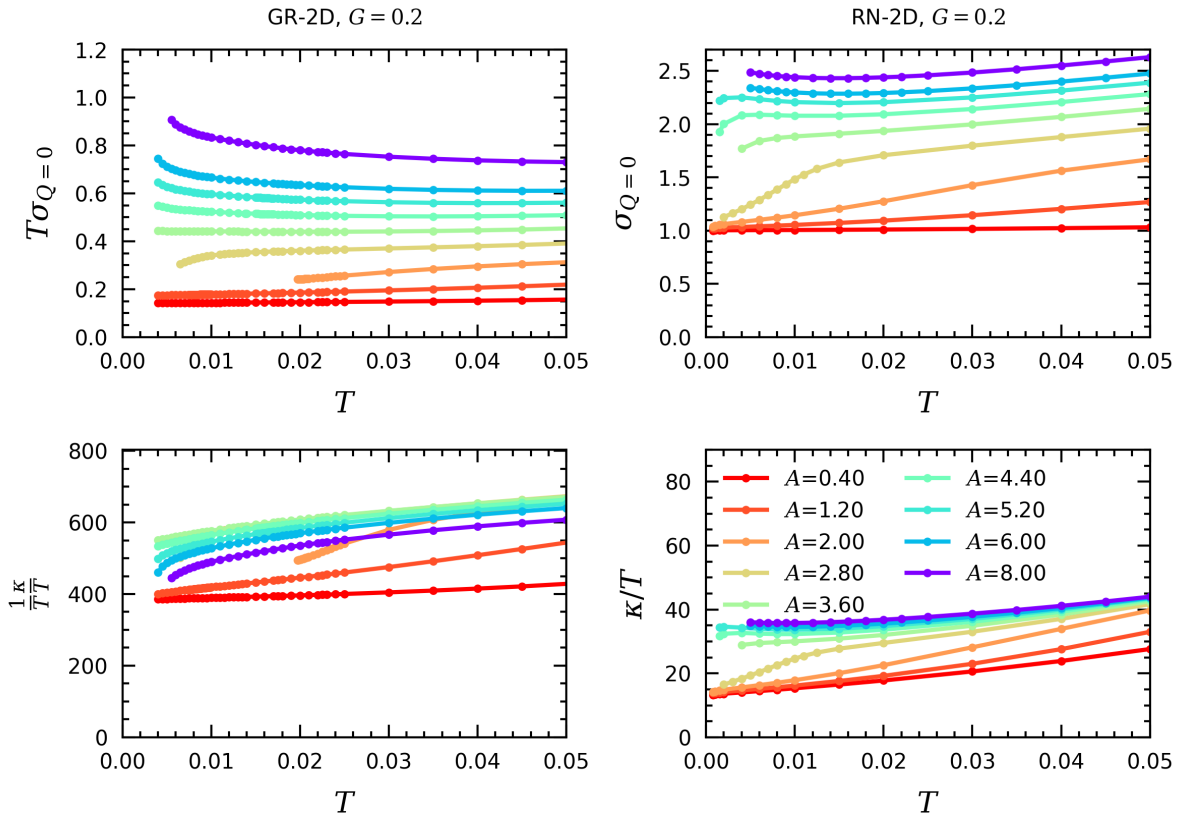

Figure 6.4: *$\sigma_{Q=0}$ and κ calculated according to (2.2) and (2.3), from the other conductivities.*

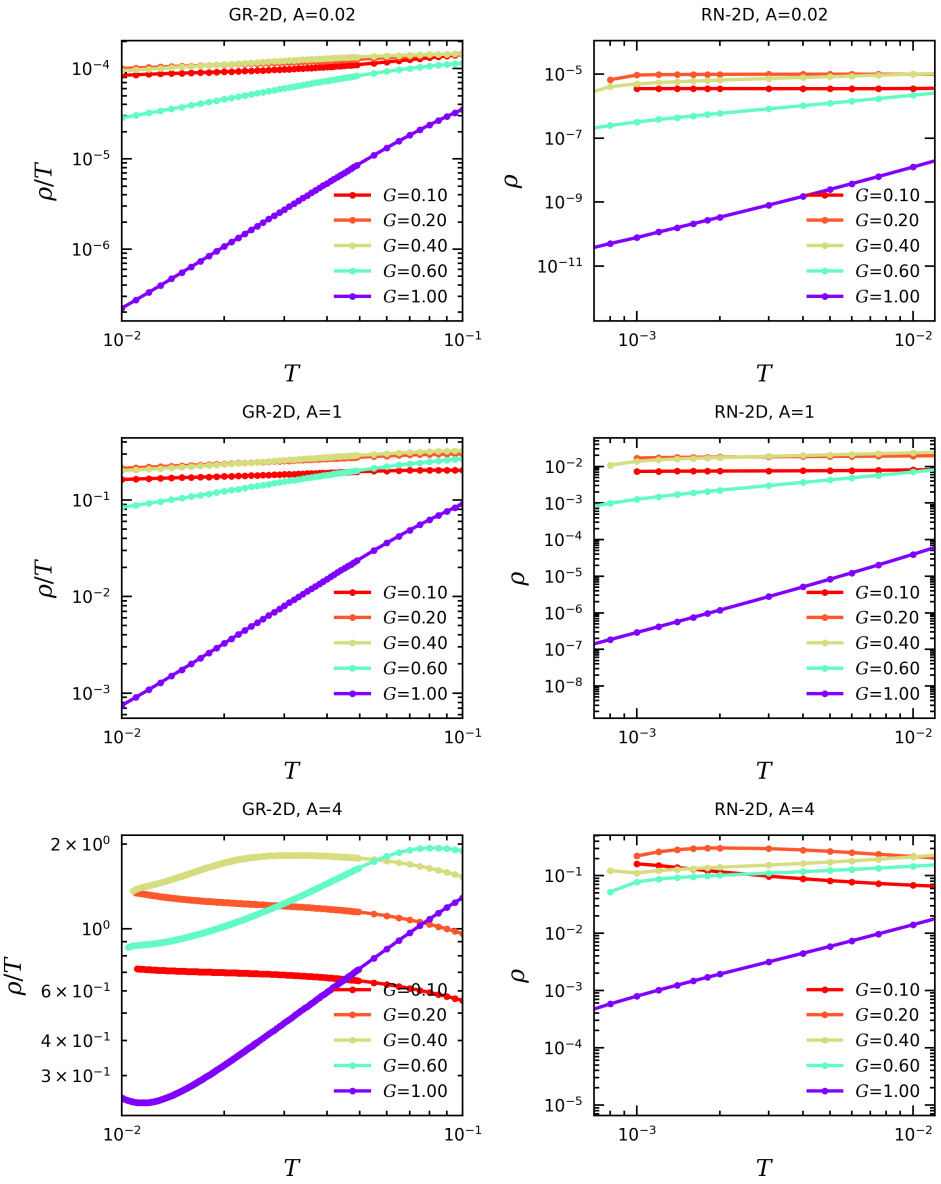

Figure 6.5: *The resistivity scaling of the GR metal (left) and RN metal (right) for different values of G. For the weak lattices we see the power-law scaling regime kicking in between $G = 0.4\mu$ and $G = 0.6\mu$.*

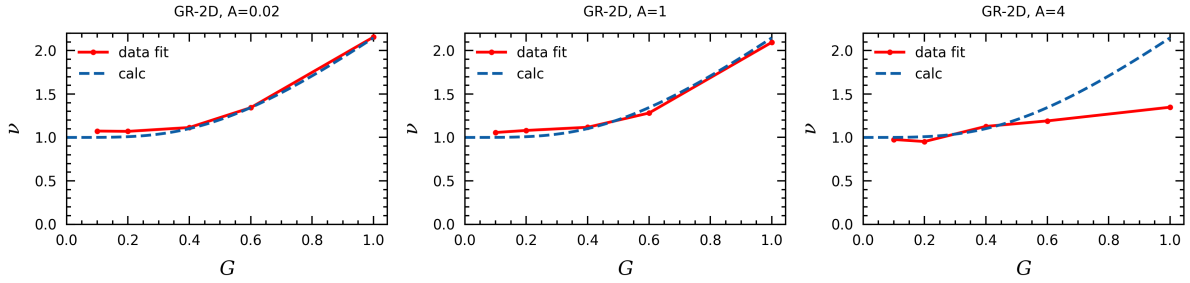

Figure 6.6: *Fitting of (4.13) (blue) to the data (red) for different lattice strengths.*

Version of June 30, 2022– Created June 30, 2022 - 14:02

Chapter 7

Discussion

7.1 Discussion

The first law of thermodynamics $\mathcal{E} + \mathcal{P} = Ts + \mu n$ seems to be satisfied for weak lattices, but starts to deviate for larger lattice strengths. The RN results by S. Arend and M. Janse have a similar result to this [14]. Since they see less deviation for vanishing temperature, they suggest that the deviation could be caused by the Ts term, which might need corrections due to the pathological entropy. We however do not have this pathology and the large deviation and should not necessarily be related to the temperature-entropy term. Furthermore recent research [50] suggests that the inclusion of a dilation field should add an additional term to the first law of thermodynamics. One might expect a larger deviation from unity $\frac{\mathcal{E}+\mathcal{P}}{Ts+\mu n}$ then we see in Figure 6.1. This is however still being researched and depends a lot on the form of the dilaton field.

We have shown that Gubser-Rocha metal with an explicit umklapp potential, experience a resistivity linear in temperature in the hydrodynamic regime. This is consistent with the predictions based on hydrodynamic arguments and suggests that this metal could be a good model for the strange metal which experiences the same temperature scaling of the resistivity.

If we would assume the different conductivities to be perfectly of the Drude form, the should only differ by factor $\frac{n}{s}$ like $\sigma_{Drude} = \frac{n}{s}\alpha_{Drude} = \frac{n^2}{s^2}\frac{\bar{\kappa}_{Drude}}{T}$. Since the entropy is linear in temperature and the thermodynamics show that $\frac{s}{n} \sim T$, the Drude conductivities should all differ by factors of T. Since we expect the resistivity to be linear in T, we plotted σT to see constant lines. If all the conductivities are dominated by Drude, this should mean that α and $\frac{1}{T}\frac{\bar{\kappa}}{T}$ should also be constant in temperature. Figure 6.3 confirms this and this would suggest that the conductivities are dominated by Drude. However as can be found in the thesis of O. Moors[51], a consistent Drude fit has not been found.

We then note from Figure 6.4 that $\sigma_{Q=0}$ actually changes a lot when varying A. Meanwhile κ stays of the same order. We also see that for large A the conductivities are dominated by the contributions from $\sigma_{Q=0}$ and κ, while in the almost homogeneous case they are neglectable. We are still trying to understand the meaning of these two quantities and in general the incoherent contributions, but we might be on our way. Recently J. Zaanen

made a claim on universality governing the diffusivity. If thermal diffusivity of quantum supreme matter is caused by quantum chaos and set by the butterfly velocity, this also predicts a scaling for κ in temperature. By the Einstein relations, the thermal diffusivity and κ are related by the specific heat, which when computed results in the scaling $\kappa \sim T^2$. The the momentum diffusivity in quantum supreme matter is set by the minimal viscosity. Both diffusivities scale the same and the claim is that there is just one universal diffusivity, governing both thermal and momentum diffusivity. This then results in an explicit expression for the butterfly velocity and for the thermal conductivity κ. It explains why κ is very small at low temperatures for the homogeneous GR case. Next one could relate all incoherent contributions conductivities to this κ, explaining why also these are small at low temperatures and weak lattices. This is however still a topic of being explored by the Leiden Quantum Matter Theory Group.

Furthermore the data showed a confirmation of the hydrodynamic regime for $G < \xi_\eta^{-1}$. This makes all the data of the conductivities used for confirmation of the linear in temperature resistivity and the shear length saturation accountable, since that data was retrieved at $G = 0.2\mu$, clearly in the hydrodynamic regime. Outside the hydrodynamic regime, we found a confirmation of the power-law regime described by (4.13) for $G > \xi_\eta^{-1}$. Meanwhile Figure 6.3 shows a saturation in the conductivities for increasing lattice strength. Combining these results we find an agreement with the limit of the shear length to the correlation length for DC transport. This was also found to be true for the RN metal as found by S. Arend and M. Janse [14, 15]. However, still unpublished results of the optical conductivities show that this is not yet the full story.

7.2 Beyond This Thesis

As mentioned before, an elaborate analysis of fitting Drude theory to the data of the GR metal can be found in the thesis of O. Moors [51]. S. Arend and M. Janse looked at DC transport in the RN metal [14, 15]. They also looked at the dependence of the magnetic field, which gave rise to transversal conductivities. Including a magnetic field to the GR metal would be an interesting point of research, which could immediately be compared to the results from the RN metal.

Another important topic of research is the AC transport. This is currently being investigated in the Quantum Matter Theory Group in Leiden. Specifically as start has been made on AC transport with magnetic field in the RN metal by O. Moors [51]. The optical conductivities for both the RN metal and GR metal at low temperatures is being looked at by the rest of the research group. This is a rich regime. It is modeled for both an explicit lattice, like we do, and for weakly broken translation invariance in a perturbative manner. Specifically the optical conductivities of the GR metal with weakly broken translation symmetry can be found in the thesis of J. Aretz [52].

Furthermore, the influence of the dilaton field to the thermodynamics should be better understood and also how the lattice affects the thermodynamics. As the current understanding of the addition of the dilaton field is developing, data produced by our group can be used to falsify the developments. The Gubser-Rocha solution for an EMD background does make constraints on the dilation parameterized by a scalar. Ideally one would want to do computations for a more general solution, but this might not exist in an analytical

form. One could then also generate data for other values of z and θ. Such a setup, if found, would likely be more computationally demanding and the numerical limits will need to be pushed even more.

One of the goals of the research group is to bring all this theory one day to the lab. Hopefully the understanding gathered by the efforts of the group will be experimentally testable on strange metals in the near future.

Acknowledgments

In this thesis I would like to take some time and space to thank the people I have had the chance to work with. First of all thanks to my supervisors Koenraad Schalm and Jan Zaanen; leading and unique research group, discussing new ideas and explaining physics and methods of research. Then I would like to thanks Floris Balm, creator of holocode behind the computational efforts, for providing all necessary codes, support and answers to our questions. I would thanks Ole Moors, for being the partner in our research. We worked together and together we would stumble upon problems, have discussions and interpret results. Next I would like to thanks Joost Aretz, although working on some different topics, towards the end of the project we got more overlap. We could discuss a lot of questions we had during our time in our shared office space. Also thanks to Sam Arends and Martijn Janse, as our predecessors in the group, they helped to get us going an familiarizing us with some of the topics. They were always ready to answer our questions and stayed involved even after their graduation. Lastly I would like to thank the research group as a whole for giving me the opportunity to experience the discussions taking place on the frontiers of science.

Bibliography

[1] H. Kamerlingh Onnes, *Further experiments with liquid helilum. C. On the change of electric resistance of pure metals at very low temperatures etc. IV. The resistance of pure mercury at helium temperatures*, *Commun. Phys. Lab. Univ. Leiden* **120b** (1911). Reprinted in *Proc. K. Ned. Akad. Wet.* **13** 1274-1276 (1911). ↑§1

[2] J. Bardeen, L.N. Cooper and J.R. Schrieffer, *Microscopic Theory of Superconductivity*, *Physical Review* **106** 162 (1957). ↑§1

[3] J. Bardeen, L.N. Cooper and J.R. Schrieffer, *Theory of superconductivity*, *Physical Review* **108** 1175 (1957). ↑§1

[4] W.L. McMillan, *Transition Temperature of Strong-Coupled Superconductors*, *Physical Review* **167** 331 (1968). ↑§1

[5] M.L. Cohen and P.W. Anderson, *Comments on the Maximum Superconducting Transition Temperature*, *AIP Conference Proceedings* **4** (1972). No citations.

[6] B. Keimer, S.A. Kivelson, M.R. Norman, S. Uchida and J. Zaanen, *From quantum matter to high-temperature superconductivity in copper oxides*, *Nature* **518** 179 (2015). ↑§1

[7] N.W. Ashcroft, *Metallic Hydrogen: A High-Temperature Superconductor?*, *Physical Review Letters* **21** 1748 (1968). ↑§1

[8] A.P. Drozdov, M.I. Eremets, I.A. Troyan, V. Ksenofontov and S.I. Shylin, *Conventional superconductivity at 203 kelvin at high pressures in the sulfur hydride system*, *Nature* **525** 73 (2015) [arXiv:1506.08190]. ↑§1

[9] J.G. Bednorz and K.A. Müller, *Possible high Tc superconductivity in the Ba-La-Cu-O system*, *Zeitschrift für Physik B Condensed Matter* **64** 189 (1986). ↑§1

[10] J. Zaanen, *The Classical Condensates: from Crystals to Fermi-liquids*, 1996. ↑§1, §2.4

[11] J. Zaanen, *Lectures on quantum supreme matter*, arXiv:2110.00961. ↑§1, §1.1, §2.4, §2.4, §4.1, §4.1

[12] G. Mirarchi, G. Seibold, C. Di Castro, M. Grilli and S. Caprara, *The Strange-Metal Behavior of Cuprates*, *Condensed Matter* **7** 29 (2022). ↑§1.2

[13] J.M. Maldacena, *The Large N Limit of Superconformal Field Theories and Supergravity*, *Advances in Theoretical and Mathematical Physics* **2** 231 (1998) [arXiv:hep-th/9711200]. ↑§1, §3.1

[14] S.C. Arend, *Magneto-Transport of a Reissner-Nordström Holographic Metal*, Master's thesis, Leiden University, Leiden, 2022. ↑§1, §5.1.1, §7.1, §7.2

[15] M.A. Janse, *Magnetotransport and dissipation in locally quantum critical metals subject to umklapp potentials*, Master's thesis, Leiden University, Leiden, 2021. ↑§1, §5.1.1, §7.1, §7.2

[16] L. Onsager, *Reciprocal Relations in Irreversible Processes. I.*, *Physical Review* **37** 405 (1931). ↑§2.1

[17] S.H. Simon, *The Oxford Solid State Basics*, Oxford University Press, Oxford (2013). ↑§2.2

[18] J. Zaanen, *Planckian dissipation, minimal viscosity and the transport in cuprate strange metals*, *SciPost Physics* **6** 61 (2019) [arXiv:1807.10951]. ↑§2.4, §4.4

[19] P. Ball, *First quantum computer to pack 100 qubits enters crowded race*, *Nature* **599** 542 (2021). ↑§2.4

[20] J.D. Bekenstein, *Black holes and the second law*, *Lett. Nuovo Cimento* **4** 737 (1972). ↑§3.1

[21] S.W. Hawking, *Particle creation by black holes*, *Commun.Math. Phys* **43** 199 (1975). ↑§3.1

[22] G. 't Hooft, *Dimensional Reduction in Quantum Gravity*, *AIP Conf. Proc. C* **930308** 284 (1993) [arXiv:gr-qc/9310026]. ↑§3.1

[23] L. Susskind, *The world as a hologram*, *Journal of Mathematical Physics* **36** 6377 (1995) [arXiv:hep-th/9409089]. ↑§3.1

[24] L. Susskind, *The Black Hole War: My Battle with Stephen Hawking to Make the World Safe for Quantum Mechanics*, Little, Brown and Company (7, 2008). ↑§1

[25] S.S. Gubser, I.R. Klebanov and A.M. Polyakov, *Gauge Theory Correlators from Non-Critical String Theory*, *Physics Letters B* **428** 105 (1998) [arXiv:hep-th/9802109]. ↑§3.4

[26] E. Witten, *Anti De Sitter Space And Holography*, *Advances in Theoretical and Mathematical Physics* **2** 235 (1998) [arXiv:hep-th/9802150]. ↑§3.4

[27] M. Baggioli, *A Practical Mini-Course on Applied Holography*, arXiv:1908.02667. ↑§3.1

[28] J. Zaanen, Y. Liu, Y.-W. Sun and K. Schalm, *Holographic Duality in Condensed Matter Physics*, Cambridge University Press (2015), doi:10.1017/cbo9781139942492. ↑§3.1

Version of June 30, 2022– Created June 30, 2022 - 14:02

[29] J. McGreevy, *Holographic duality with a view toward many-body physics*, *Advances in High Energy Physics* **2010** (2010) [arXiv:0909.0518]. ↑§3.2

[30] S.S. Gubser and F.D. Rocha, *Peculiar properties of a charged dilatonic black hole in AdS_5*, *Phys. Rev. D* **81** (2010) [arXiv:0911.2898]. ↑§3.8, §4.1, §5.1.2

[31] C.M. Varma, P.B. Littlewood, S. Schmitt-Rink, E. Abrahams and A.E. Ruckenstein, *Phenomenology of the normal state of Cu-O high-temperature superconductors*, *Physical Review Letters* **63** (1989). ↑§4.1

[32] M. Mitrano, A.A. Husain, S. Vig, A. Kogar, M.S. Rak, S.I. Rubeck et al., *Anomalous density fluctuations in a strange metal*, *Proceedings of the National Academy of Sciences of the United States of America* **115** 5392 (2018). ↑§4.1

[33] C. Charmousis, B. Goutraux, B.S. Kim, E. Kiritsis and R. Meyer, *Effective holographic theories for low-temperature condensed matter systems*, *Journal of High Energy Physics* **2010** 151 (2010) [arXiv:1005.4690]. ↑§4.1

[34] B. Goutéraux and E. Kiritsis, *Generalized holographic quantum criticality at finite density*, *Journal of High Energy Physics* **36** 1 (2011) [arXiv:1107.2116]. ↑§4.1

[35] L. Huijse, S. Sachdev and B. Swingle, *Hidden Fermi surfaces in compressible states of gauge-gravity duality*, *Physical Review B* **85** 035121 (2012) [arXiv:1112.0573]. ↑§4.1

[36] J. Zaanen, *Why the temperature is high*, *Nature* **430** 512 (2004). ↑§4.3

[37] G. Policastro, D.T. Son and A.O. Starinets, *Shear Viscosity of Strongly Coupled N=4 Supersymmetric Yang-Mills Plasma*, *Physical Review Letters* **87** 081601 (2001) [arXiv:hep-th/0104066]. ↑§4.3

[38] P.K. Kovtun, D.T. Son and A.O. Starinets, *Viscosity in strongly interacting quantum field theories from black hole physics*, *Physical Review Letters* **94** 111601 (2005) [arXiv:hep-th/0405231]. ↑§4.3

[39] W. Busza, K. Rajagopal and W. van der Schee, *Heavy Ion Collisions: The Big Picture and the Big Questions*, *Annual Review of Nuclear and Particle Science* **68** 339 (2018) [arXiv:1802.04801]. ↑§4.3

[40] S. Martin, A.T. Fiory, R.M. Fleming, L.F. Schneemeyer and J.V. Waszczak, *Normal-state transport properties of Bi2+xSr2-yCuO6+δ crystals*, *Physical Review B* **41** 846 (1990). ↑§4.4

[41] R.A. Davison, K. Schalm and J. Zaanen, *Holographic duality and the resistivity of strange metals*, *Physical Review B* **89** 245116 (2014) [arXiv:1311.2451]. ↑§4.4

[42] N. Iqbal, H. Liu and M. Mezei, *Semi-local quantum liquids*, *Journal of High Energy Physics* **2012** 86 (2012) [arXiv:1105.4621]. ↑§4.5

[43] S.A. Hartnoll and D.M. Hofman, *Locally Critical Resistivities from Umklapp Scattering*, *Physical Review Letters* **108** 241601 (2012) [arXiv:1201.3917]. ↑§4.5

[44] R.J. Anantua, S.A. Hartnoll, V.L. Martin and D.M. Ramirez, *The Pauli exclusion principle at strong coupling: holographic matter and momentum space*, *Journal of High Energy Physics* 104 (2013) [arXiv:1210.1590]. ↑§4.5

[45] S.A. Hartnoll, P.K. Kovtun, M. Müller and S. Sachdev, *Theory of the Nernst effect near quantum phase transitions in condensed matter and in dyonic black holes*, *Physical Review B* **76** 144502 (2007) [arXiv:0706.3215]. ↑§4.7

[46] S. Hartnoll, A. Lucas and S. Sachdev, *Holographic Quantum Matter*, The MIT Press, Cambridge (3, 2018), [arXiv:1612.07324]. ↑§4.7

[47] R.A. Davison and B. Goutéraux, *Dissecting holographic conductivities*, *Journal of High Energy Physics* **2015** (2015) [arXiv:1505.05092]. ↑§4.7

[48] Y. Ling, C. Niu, J.-P. Wu and Z.-Y. Xian, *Holographic Lattice in Einstein-Maxwell-Dilaton Gravity*, *Journal of High Energy Physics* 6 (2013) [arXiv:1309.4580]. ↑§5.1.2

[49] F. Balm, Ph.D. thesis, Leiden University, Leiden, 2022. ↑§5.3

[50] L. Li, *On thermodynamics of AdS black holes with scalar hair*, *Physics Letters B* **815** 136123 (2021) [arXiv:2008.05597]. ↑§7.1

[51] O. Moors, *Drude Theory in Reissner-Nordström and Gubser-Rocha Holographic Strange Metals*, Master's thesis, Leiden University, Leiden, 2022. ↑§7.1, §7.2

[52] J. Aretz, *Quasinormal Modes of Gubser-Rocha Holomatter*, Master's thesis, Leiden University, Leiden, 2022. ↑§7.2